Graphene at fluidic interfaces

Belyaeva, L.A.

Cover Page

Universiteit Leiden

The handle http://hdl.handle.net/1887/79822 holds various files of this Leiden University dissertation.

Author: Belyaeva, L.A.
Title: Graphene at fluidic interfaces
Issue Date: 2019-10-23

CHAPTER 2

Molecular caging of graphene with cyclohexane: transfer and electrical transport

Transfer of large, clean, crack- and fold-free graphene sheets is a critical challenge in the field of graphene-based electronic devices. Polymers, conventionally used to transfer two-dimensional materials irreversibly adsorb on their surface yielding a range of unwanted chemical functions and contaminations. An oil-water interface represents an ideal support for graphene. Cyclohexane, the oil phase, protects graphene from mechanical deformation and minimizes vibrations of the water surface. Remarkably, cyclohexane solidifies at 7°C forming a plastic crystal phase molecularly conforming graphene, preventing the use of polymers, and thus drastically limiting contamination. Graphene floating at the cyclohexane/water interface exhibits improved electrical performances allowing for new possibilities of in situ, flexible sensor devices at a water interface.

2.1. Introduction

For years now, long chain polymers are used to prevent cracking and to preserve the two-dimensional nature of graphene during transfer.[1–6] Because of their macromolecular structures, polymers can hardly be removed from the graphene surface:[7–9] they irreversibly adsorb and modify the chemical and physical properties of graphene.[10,11] Instead of using polymers, so-called polymer-free transfer techniques use special frames and holders to keep the sheet integrity of graphene.[12,13] Very recently a biphasic system composed of an aqueous solution of ammonium persulfate and hexane has been employed to transfer clean graphene.[14] Transfers not involving polymers, however, are widely known to induce cracks as graphene is a macroscopic sheet that has to be mechanically maintained while and after the underlying growth catalyst is etched. Polymers are known to protect graphene from cracking and folding at the cost of extensive contamination, highlighting the need for a top phase that can be solidified without the use of polymerization reactions. This chapter demonstrates that cyclohexane can operate similarly to a polymer support, however, without inducing major contamination on the graphene surface. The caging of graphene at a cyclohexane/water interface harvests nonpolar binding interactions between graphene and an organic liquid to maintain graphene flat, while still permitting the etching of the growth catalyst from the etchant bottom aqueous phase. Such organic-aqueous interfaces have been used for separating and extracting products of chemical reactions,[15,16] and have the potential for *in situ* graphene functionalization[17,18] and electrochemistry.[19,20]

Here, the fluidic interface – that is two immiscible liquids with graphene in between – allows to mechanically and continuously relax graphene from stresses induced during etching, preventing the formation of the wrinkles always observed in conventional graphene transfers. In addition, the surface tension forces at the cyclohexane-water interface damp down low amplitude vibrations therefore preventing graphene from cracking, which always occur when graphene floats on the surface of water without a polymer support.

Cyclohexane was employed as the organic phase because of several important physical properties: i) cyclohexane is immiscible with water, ii) cyclohexane conforms the surface of graphene during copper etching at room temperature, and most importantly, iii) cyclohexane solidifies at 7°C forming a plastic crystal phase supporting graphene once the copper is etched. The soft gel-like structure of the plastic crystal phase of cyclohexane (this chapter only considers the high-temperature solid phase of cyclohexane, stable between -87°C and melting at 7°C, as shown in Figure 2.1a) conforms the surface of graphene preventing mechanical damaging with minimum contamination and handling, because only cooling down from room temperature to 0-7°C is needed to solidify the cyclohexane phase. After transfer to the final substrate, the residues of cyclohexane are easily removed by melting and evaporating cyclohexane at room temperature.

Such biphasic platform also yields intact graphene with high electrical performance as cyclohexane is chemically benign and completely removable from graphene: for the first time, probing the electric field-effect properties of graphene at the biphasic interface showed a charge carrier mobility reaching $\mu=3{,}470$ cm^2/Vs, a value superior to — for example — the same batch of graphene transferred on a Si/SiO$_2$ ($\mu=2{,}180$ cm^2/Vs) and epoxy substrates ($\mu=1{,}505$ cm^2/Vs).

2.2. Results and Discussion

2.2.1. Interfacial caging of graphene: the concept

Water and cyclohexane are immiscible (solubility of cyclohexane in water is 0.006% at 25°C; solubility of water in cyclohexane is 0.01% at 20°C) and ammonium persulfate – the copper etchant – is insoluble in cyclohexane, minimizing the interchange of matter between the two phases. Once placed at the cyclohexane-air interface, the graphene/copper sample sinks to the cyclohexane/water interface and floats there exposing graphene to the cyclohexane phase and copper to the etchant solution (see Figure 2.1b and c).

Once the copper is completely etched graphene remains floating in between the two phases (Figure 2.1b). Water and cyclohexane apply pressure on both sides of graphene, and serve as a firm, but flexible shell conforming the surface of graphene.
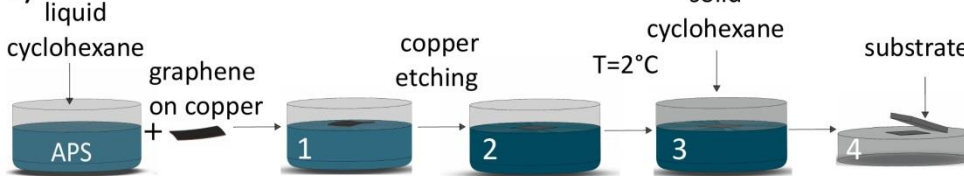

Figure 2.1. The cyclohexane and water interface for graphene caging and biphasic transfer. a) Temperature dependence of the state of matter for cyclohexane and water. In the temperature (T) range -87°C < T < 7°C cyclohexane forms a plastic crystal phase, whereas water is liquid at temperatures above 0°C. b) Interfacial caging employed at temperatures above 0°C. Biphasic transfer is carried at temperatures between 0°C and 7°C in which cyclohexane is a plastic crystal and water is liquid. c) Illustration depicting the interfacial transfer process. Graphene on copper is placed in a biphasic mixture of water and cyclohexane at room temperature (1), the copper is etched using ammonium persulfate in water (2), the solution is then cooled down to 2°C until the cyclohexane phase solidifies (3), and the cyclohexane phase with graphene adsorbed is transferred onto a substrate (4). In a last step the sample is kept at 2°C until the cyclohexane sublimates completely from the solid to the gas phase.

2.2.2. Interfacial transfer process

After copper is etched, the biphasic oil-water mixture is cooled down to 2°C (Figure 2.1c). At 2°C cyclohexane solidifies and forms a solid mold on the top-side of the graphene surface. The solid cyclohexane phase with adsorbed graphene can be separated from the etchant and rinsed with cold water at 2°C to remove residues of etchant. The cyclohexane mold is then taken out and placed on the final substrate that has been preliminarily cooled down. The cyclohexane/graphene/substrate stack is then placed in an open container with constant temperature around 0-2°C (a box with water ice or ventilated fridge in our case). Cyclohexane kept at 2°C is volatile and sublimates gently in 15-90 minutes depending on the volume used, leaving graphene intact on the substrate. A volume ratio between the two phases of 1:1 was used, typically 10 mL of 0.5M APS in water and 10 mL of cyclohexane. Cyclohexane was then left to evaporate overnight at a temperature ranging from 0-4°C, typically in an ice-water bath or in a ventilated fridge.

An alternative is to directly deposit the substrate on the copper foil covered with graphene at the cyclohexane-water interface. Next, cyclohexane is solidified by cooling down the biphasic mixture to 0-2°C, and the solid cyclohexane phase with the incrusted substrate with graphene is taken out of the beaker. The fact that graphene was in contact with the substrate from the very start of the transfer prevents the presence of ammonium persulfate residues between graphene and the substrate. The APS salt residues on the other side of graphene can be removed by rinsing the sample with water. The rinsing has to be done slowly to maintain the 0-2°C as it can cause melting of cyclohexane and the detachment of graphene.

2.2.3. Crucial to freeze cyclohexane

To demonstrate the importance of freezing cyclohexane, three control transfer experiments were performed. First, cyclohexane was not frozen and the graphene floating at the interface was directly "fished-out", that is contact-

stamped, using a silicon wafer. The turbulence occurring both in the cyclohexane phase and in the etchant phase due to the insertion of the wafer broke the graphene apart. In a second experiment, a wafer was placed on copper/graphene prior etching without freezing the cyclohexane. In both cases, no graphene was transferred to the substrate, which therefore, indicated that solidification of cyclohexane prior transferring graphene was an essential step. In a last experiment a silicon wafer was placed on copper/graphene floating on the etchant without using cyclohexane: again, no graphene was found on the wafer after the transfer.

2.2.4. Integrity and quality of graphene transferred using interfacial caging

The properties of graphene (continuality, density of cracks, size of wrinkles, density of wrinkles) transferred using interfacial caging were compared with: i) the most commonly used PMMA-based polymer-assisted transfer (Figure 2.2b),[2,3] ii) the potentially most "clean" method, which is introduced here as "contact-stamping", where graphene is transferred by pushing the substrate down into water towards a floating graphene flake, and iii) the hexane-assisted transfer (see Appendix 1 for more details).[14] The PMMA polymer (i.e., poly(methylmethacrylate)) protects and conforms the surface of graphene and therefore allows transferring large and continuous areas of graphene (Figure 2.2b). Polymer residuals, however, are inevitable, contaminating the surface of graphene.[11] In contrast, contact-stamping and hexane-assisted transfer methods result in cleaner, but discontinuous graphene samples with multiple irregularities (foldings, wrinkles, cracks, etc., see Figure 2.2c-d). Interfacial caging, however, yields large and continuous graphene sheets if transferred onto Si/SiO$_2$ substrates (Figure 2.2a) with negligible folding and almost no micrometer-scale wrinkles.

The optical micrographs of graphene transferred with PMMA and interfacial caging are similar (Figure 2.2a versus Figure 2.2b). Among all the existing transfer methods, interfacial caging and the PMMA-assisted method showed least amounts of cracks (Figure 2.2a, b). Graphene transferred by contact stamping is less uniform (cracked) and has a higher density of wrinkles, even more evident on the magnified optical micrographs (Figure 2.2c, inset). Those wrinkles likely

originate from the moment when graphene floating on the etchant is brought in contact with the wafer during stamping. Contact stamping and hexane-assisted transfer methods yield similar graphene morphologies: when graphene is scooped out of the biphasic system, the graphene brakes into smaller pieces and therefore becomes largely wrinkled and cracked (Figure 2.2c and d).

The Raman spectra of graphene transferred on silicon wafers using the interfacial caging, the PMMA-assisted method and the contact stamping are similar, showing the characteristic peaks of monolayer graphene (Figure 2.2e, Table 2.1): a sharp 2D peak (I_{2D}/I_G ratio of 2.4 for interfacial caging, 1.4 for PMMA-assisted and 2 for contact stamping methods respectively; with a FWHM for the 2D peak of 30 cm^{-1}), fitting one Lorentz function indicating the presence of monolayer graphene,[21] and a negligible D peak suggesting almost no defects in the graphene lattice (I_D/I_G ratio of 0.1 for interfacial caging and the PMMA-assisted transfer methods, and I_D/I_G ratio of 0.2 for contact stamping).[21] These ratios indicate that the graphene transferred using interfacial caging has a defect density similar to the graphene samples transferred using PMMA and contact-stamping.

Table 2.1. Raman characteristics of graphene transferred by interfacial caging, PMMA-assisted and contact stamping transfer methods

	D peak position, cm^{-1}	G peak position, cm^{-1}	2D peak position, cm^{-1}	I_D/I_G	I_{2D}/I_G	FWHM, cm^{-1}
Interfacial caging	1343	1587	2686	0.1	2.4	30
PMMA-assisted	1345	1587	2687	0.1	1.4	26
Contact stamping	1343	1587	2687	0.2	2	33

Remarkably, if interfacial caging is used to fabricate suspended graphene areas (~2 μm^2) on a porous substrate, a full coverage is achieved in large scale. Figure 2.2f shows scanning electron micrographs images of the samples transferred using the interfacial caging on holey transmission electron microscope grids. Particularly, free-standing graphene membranes are free from wrinkles, tears and visible contamination (see Figure 2.2f).

Graphene transferred to quantifoil grids also showed no traces of cyclohexane, as shown by TEM in Figure 2.2g. Upon exposure to the electron beam of the TEM, contamination on the graphene surface accumulates quickly (in the course of 40 s) in the area exposed to the electron beam, and is seen as amorphization in the diffraction patterns of graphene.[22] In contrast, our sample exhibited almost no change in diffraction patterns taken over 15 minutes, which indicates, that no noticeable contamination took place on graphene surface (Figure 2.2g).
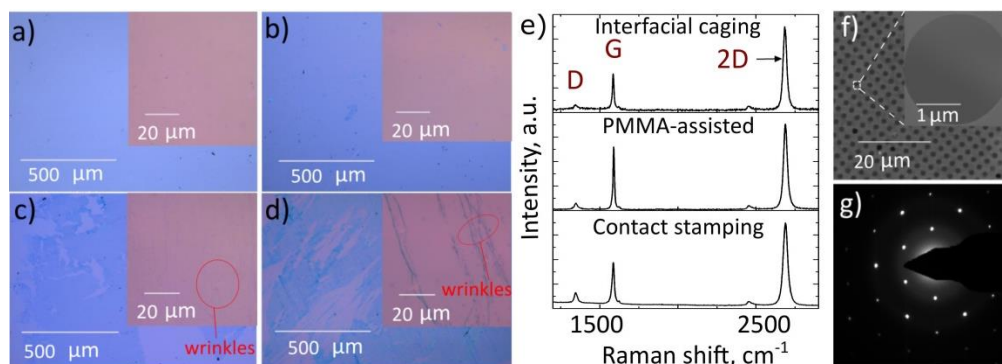

Figure 2.2. Comparison of the interfacial caging transfer with conventional transfer methods (PMMA-assisted, contact stamping, hexane-assisted). a) Optical micrograph of graphene transferred using interfacial caging with solidified cyclohexane. b) Optical micrograph of graphene transferred using the PMMA-assisted method. c) Optical micrograph of graphene transferred using contact stamping. d) Optical micrograph of graphene transferred using the hexane-assisted method.[14] e) Raman spectra of graphene transferred onto silicon wafers using interfacial caging, PMMA-assisted and contact stamping. f) Scanning electron micrograph of graphene transferred to a quantifoil electron microscopy grid using interfacial caging. Inset: zoomed-in view of graphene free-standing on top of a hole on the grid – no contamination, cracks and folding's are visible. g) Diffraction pattern of graphene transferred with interfacial caging. TEM was carried with a 300kV electron beam focused to a 100 nm probe size, spot size 3, C_2 apperture of 20 mm on a FEI Titan.

Graphene transferred by interfacial caging (Figure 2.3a) was further studied using atomic force microscopy (AFM) and compared with the results obtained with conventional transfer methods (Figure 2.3b-d). A typical AFM image of graphene transferred to a silicon wafer using PMMA shows multiple features that

correspond to wrinkles, PMMA residues, dust particles and other topological features (Figure 2.3b).[8,9,11] The wrinkles are denser and larger for PMMA transferred graphene (3-10 nm in height) than for interfacial caging (below 2 nm, see Figure 2.3a and 2.3b). Contact stamped graphene, as expected, exhibits repetitive patterns with parallel wrinkles (white lines with a length of a few micrometers and heights up to 10 nm, see Figure 2.3c), a result in agreement with the optical micrographs of the same samples (Figure 2.2c). The surface of the hexane-transferred graphene also contains wrinkles with heights of 2-5 nm, which are smaller than for contact stamped graphene, and larger than for the samples transferred using interfacial caging (Figure 2.3d). The large particles that are seen in all AFM images, for all three samples are dust particles and possibly copper etchant crystals/residuals. Those contaminants are very difficult to avoid when working under atmospheric conditions, and not in a cleanroom.
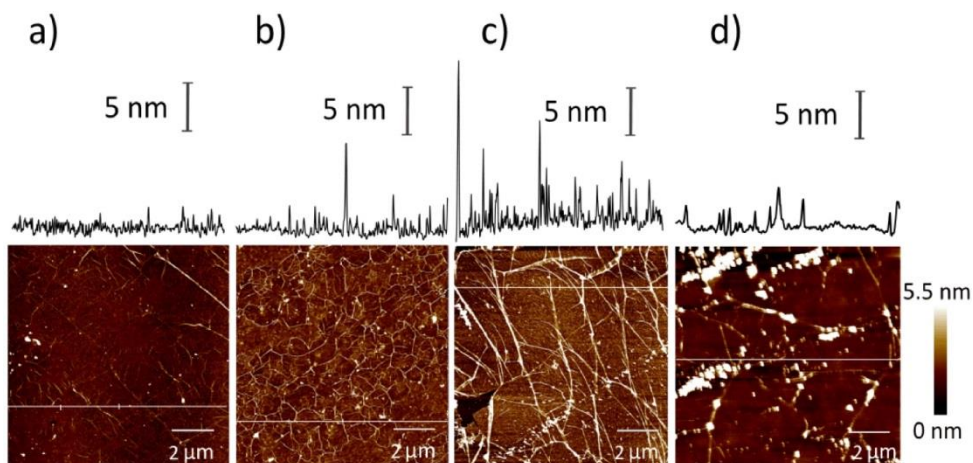

Figure 2.3. AFM images and height profiles of graphene samples transferred to a silicon wafer using interfacial caging and other conventional transfer methods. a) Interfacial caging method. b) PMMA-assisted method. c) Contact stamping method. d) Hexane-assisted transfer method.[14] The top panel in each image shows the height profile along the line (in white) highlighted in the main image.

2.2.5. Biphasic electrolyte-gated graphene field-effect transistor

In order to confirm that the interfacial transfer procedure yields intact graphene with high electrical performance, the electric field-effect of graphene at the biphasic interface was examined. For the device fabrication, while graphene was

floating at the organic/water interface, the source and drain electrodes (25 μm thick copper) were protected by using PMMA against the etchant, leaving the upper surface available to electrically contact graphene after etching (Figure 2.4b, top) with needle electrodes. As a control, graphene devices on an epoxy substrate and on a Si/SiO$_2$ substrate were fabricated.[23] Ag/AgCl reference electrodes were used as the electrolyte gate. The conductance (G) versus gate voltage (V$_{ref}$) curves of graphene are shown in Figure 2.4a.
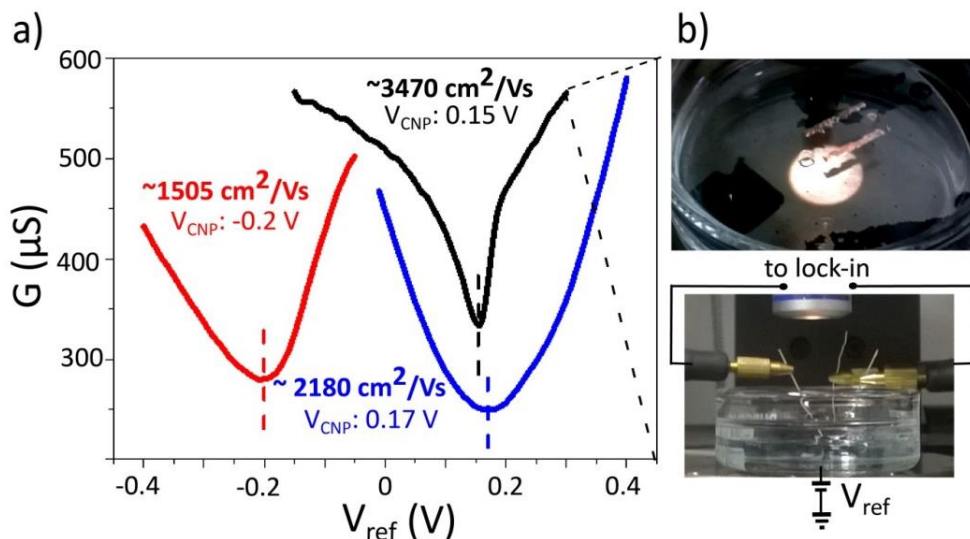

Figure 2.4. Electrical characterization of graphene at a cyclohexane/water interface. a) Electrolyte gate voltage (V_{ref}) dependent sheet conductance (G) of polymer-free graphene at a cyclohexane-water interface (black), on an epoxy substrate (red) and on a Si/SiO$_2$ substrate (blue). The gate voltage of the charge neutrality point V_{CNP} is 0.15 V for the graphene at the cyclohexane-water interface, -0.2 V on an epoxy substrate and 0.17 V for the graphene on Si/SiO$_2$. b) Photographs of the experimental setup used for probing the electronic properties of graphene at the water/cyclohexane interface: top-view (top) and side-view (bottom). As graphene floats at the organic/water interface, a bias voltage applied between the source and drain electrodes (V_{SD}) was applied between the two source and drain copper electrodes (25 μm thick Cu).

Significantly higher carrier mobility were measured for graphene floating at the water/cyclohexane interface (~3470 cm^2/Vs, ~1940 cm^2/Vs for holes and ~5000 cm^2/Vs for electrons; see Figure 2.4a), compared to ~1505 cm^2/Vs (~940 cm^2/Vs for holes and ~2070 cm^2/Vs for electrons) on the epoxy substrate and ~2180 cm^2/Vs (~1840 cm^2/Vs for holes and ~2520 cm^2/Vs for electrons) on the Si/SiO$_2$

substrate. Consequently, in the interfacial configuration the electrical properties of graphene are better than for graphene on substrates. The observed reduction in mobility after transfer onto epoxy or Si/SiO$_2$ (but with electrical properties comparable to CVD graphene transferred to Si/SiO$_2$ substrates using a PMMA – assisted method, i.e. ~100-1400 cm^2/Vs,[24] ~1100 cm^2/Vs [25]) suggests substrate scattering. The observed higher charge carrier mobilities in the case of caged graphene can be due to the fact that graphene is cleaner because of the absence of polymer contamination. The results, however, were not compared to free-standing or h-BN encapsulated graphene transistor devices, which exhibit very high carrier mobilities by removing any possible substrate scattering effects such as the one induced, for example, by Si/SiO$_2$ substrates. Important to mention, that depending on the quality of the CVD graphene, the floating graphene devices tend to break if the CVD graphene contains too many defects.

This work introduced interfacial caging and compared the performance of graphene with the most employed graphene transfer methods. The results are summarized in Table 2.2.

Table 2.2. Comparative analysis of graphene samples transferred with interfacial caging, PMMA, contact stamping and the hexane-assisted method.

	Interfacial caging method	PMMA-assisted method	Contact stamping	Hexane-assisted method
Continuality	full coverage of the wafer	full coverage of the wafer	partial coverage of the wafer	partial coverage of the wafer
Density of cracks	low	low	high	high
Size of wrinkles	2-3 nm high, 0.5-2 µm long	2-15 nm high, up to 10 µm long	>15 nm high, >10 µm long	2-15 nm high, up to 10 µm long
Density of wrinkles	low	high	high	medium

For polymer-based transfer using PMMA, graphene is supported by a polymer, promoting a stable mold so that further handling and lithography is possible. The polymer maintains the integrity of graphene, conforms the graphene surface and prevents graphene from forming large wrinkles. PMMA, however, conforms the catalyst, which is typically rough hence resulting in wrinkles after transfer. Another drawback of using polymers (PMMA or others) for transfer is the unavoidable presence of polymer residues on graphene, which remains even after several annealing steps. Contact stamping and hexane-assisted transfer result in cleaner, but largely cracked and wrinkled graphene.

Interfacial caging allows, on one hand, to softly support graphene from its both sides, inherently minimizing irregularities such as wrinkles and foldings using the difference in surface tension and capillary forces at a water/cyclohexane interface. On the other hand, cyclohexane, contrarily to PMMA, is a smaller molecule without a conjugated electron system, i.e. not prone to π-π stacking on graphene surface (such as benzene for example), which together with its high volatility renders cyclohexane to be very easily removed from graphene. Additionally, interfacial caging and biphasic transfer only require cooling down graphene sample without subjecting it to harsh treatments. Big areas of graphene can be transferred without inducing defects and multiple big cracks, which was confirmed by Raman spectroscopy, optical, atomic force microscopy and scanning electron microscopy.

While interfacial caging is an appealing method for transfer applications, the technique also opens new modalities for fundamental studies of floating graphene. For lithographic purposes, however, the method may be less appealing unless a physical (non-sticky) mask is used for patterning. For the first time, our interfacial approach enables electrical measurement of electrolyte-gated graphene field-effect transistors with improved electrical performance for graphene caged at a cyclohexane/water interface. The remarkably higher carrier mobility of a floating graphene flake compared to its counterpart after transfer onto either epoxy or Si/SiO_2 substrates, suggests that the intrinsic electrical properties of graphene are largely retained presumably thanks to minimal contaminations. Such high-performance, flexible graphene transistors in a

floating configuration can be readily used for in-situ sensing, for example directly at liquid/liquid interfaces.

2.3. References

1. K. S. Novoselov, S. V. Morozov, D. Jiang, Y. Zhang, S. V. Dubonos, I. V. Grigorieva, A. A. Firsov, A. K. G. Electric field effect in atomically thin carbon films. *Science* **306,** 666–669 (2004).

2. Li, X. *et al.* Transfer of large-area graphene films for high-performance transparent conductive electrodes. *Nano Lett.* **9,** 4359–4363 (2009).

3. Suk, J. W. *et al.* Transfer of CVD-grown monolayer graphene onto arbitrary substrates. *ACS Nano* **5,** 6916–6924 (2011).

4. Wood, J. D. *et al.* Annealing free, clean graphene transfer using alternative polymer scaffolds. *Nanotechnology* **26,** 55302 (2015).

5. Gao, L. *et al.* Face-to-face transfer of wafer-scale graphene films. *Nature* **505,** 190–194 (2014).

6. Feng, Y.; Huang, S.; Kang, K.; Duan, X. Preparation and characterization of graphene and few-layer graphene. *New Carbon Mater.* **26,** 26–30 (2011).

7. Su, Y. *et al.* Polymer adsorption on graphite and CVD graphene surfaces studied by surface-specific vibrational spectroscopy. *Nano Lett.* **15,** 6501–6505 (2015).

8. Han, Y. *et al.* Clean surface transfer of graphene films via an effective sandwich method for organic light-emitting diode applications. *J. Mater. Chem. C* **2,** 201–207 (2014).

9. Hallam, T., Berner, N. C., Yim, C. & Duesberg, G. S. Strain, bubbles, dirt, and folds: a study of graphene polymer-assisted transfer. *Adv. Mater. Interfaces* **1,** 1400115 (2014).

10. Pirkle, A. *et al.* The effect of chemical residues on the physical and electrical properties of chemical vapor deposited graphene transferred to SiO_2. *Appl. Phys. Lett.* **99,** 122108 (2011).

11. Kumar, K., Kim, Y.-S. & Yang, E.-H. The influence of thermal annealing to remove polymeric residue on the electronic doping and morphological characteristics of graphene. *Carbon N. Y.* **65,** 35–45 (2013).

12. Lin, W.-H. et al. A direct and polymer-free method for transferring graphene grown by chemical vapor deposition to any substrate. *ACS Nano* **8,** 1784–1791 (2014).

13. Algara-Siller, G. *et al.* Square ice in graphene nanocapillaries. *Nature* **519,** 443–5 (2015).

14. Zhang, G. *et al.* Versatile polymer-free graphene transfer method and applications. *ACS Appl. Mater. Interfaces* **8,** 8008–8016 (2016).

15. Treybal, R. E. Liquid Extraction. *Ind. Eng. Chem.* **94,** 91–99 (1951).

16. Joshi, M. D. & Anderson, J. L. Recent advances of ionic liquids in separation science and mass spectrometry. *RSC Adv.* **2,** 5470–5484 (2012).

17. Toth, P. S., Ramasse, Q. M., Velický, M. & Dryfe, R. a. W. Functionalization of graphene at the organic/water interface. *Chem. Sci.* **6,** 1316–1323 (2015).

18. Toth, P. S., Velický, M., Ramasse, Q. M., Kepaptsoglou, D. M. & Dryfe, R. a. W. Symmetric and asymmetric decoration of graphene: bimetal-graphene sandwiches. *Adv. Funct. Mater.* **25,** 2899–2909 (2015).

19. Rodgers, A. N. J. & Dryfe, R. a. W. Oxygen reduction at the liquid-liquid interface: bipolar electrochemistry through adsorbed graphene layers. *ChemElectroChem* **3,** 472–479 (2016).

20. Feng, Y. & Chen, K. Dry transfer of chemical-vapor-deposition-grown graphene onto liquid-sensitive surfaces for tunnel junction applications. *Nanotechnology* **26,** 35302 (2015).

21. Ferrari, A. C. & Basko, D. M. Raman spectroscopy as a versatile tool for studying the properties of graphene. *Nat. Nanotechnol.* **8,** 235–246

(2013).

22. Schneider, G. F. *et al.* Tailoring the hydrophobicity of graphene for its use as nanopores for DNA translocation. *Nat. Commun.* **4,** 2619 (2013).

23. Fu, W. *et al.* High mobility graphene ion-sensitive field-effect transistors by noncovalent functionalization. *Nanoscale* **5,** 12104–10 (2013).

24. Liang, X. *et al.* Toward clean and crackless transfer of graphene. *ACS Nano* **5,** 9144–9153 (2011).

25. Song, H. S. *et al.* Origin of the relatively low transport mobility of graphene grown through chemical vapor deposition. *Sci. Rep.* **2,** 337 (2012).